

# Fatigue Design of Axially Loaded Semicircular Lugs

S. K. Tsang\*

Dowty Aerospace Los Angeles, Duarte, California 91010

A simplified procedure based on the results of finite element analysis is proposed for the design of semicircular lugs under repeated axial loading. Maximum lug stresses corresponding to different failure modes are obtained by multiplying nominal stresses by stress correction factors given by design curves. Analytical limitations associated with the finite element approach and factors that affect stress and strength are discussed. The effect of friction on lug stresses is also investigated. When properly implemented, the present design procedure is expected to provide a simple, efficient, and sufficiently accurate method for the preliminary estimation of lug stresses.

## Nomenclature

$A$	= area
$a$	= lug radius
$C_f$	= fitting factor
$D$	= inside diameter
$E$	= elastic modulus
$F$	= axial load
$f$	= stress
$K$	= stress correction factor
$K_c$	= stress concentration factor
$R$	= stress ratio
$t$	= lug thickness
$t_a$	= active thickness
$W$	= lug width
$\nu$	= Poisson ratio

### Subscripts

$A, B$	= failure locations, Fig. 1
$a$	= axial
$br$	= shear-bearing
$br_{mx}$	= maximum shear-bearing
$tmx$	= maximum tension
$tn$	= tension
$v$	= Von Mises
1, 2, 3	= principal directions

## Introduction

WHEN semicircular lugs are subjected to axial loads (see Fig. 1), failure generally occurs by one of the following modes<sup>1</sup>: 1) net section tension, 2) bearing, or 3) shear tearout along "40-deg planes."

Modes 2 and 3 are closely related and can be regarded as a single mode of failure. A popular analytical method for predicting failure loads of lugs used for aircraft mechanical connections involves multiplying the load capacity based on nominal areas by efficiency factors.<sup>1,2</sup> Such efficiency factors are also referred to as active plastic stress concentration factors and are obtained by a combination of theoretical formulation and comprehensive testing on a variety of lug shapes and materials.

While such a semiempirical method has proven relatively successful for design against limit and ultimate load failures,

its use should be discouraged for fatigue design since the data on which the method is based are obtained purely from static tests. Attempts to obtain an allowable fatigue load by scaling from the ultimate load-carrying capacity based on the ratio of operating to ultimate loads are dangerous, because static load failures of lugs are generally accompanied by considerable yielding, which makes the relationship between load and stress highly nonlinear. By contrast, fatigue failures, apart from being load-dependent, are also affected by the number of load cycles and may occur almost completely within the elastic domain.

Since lug failures in aircraft applications occur predominantly under fatigue conditions, there is a need to extend the semiempirical method<sup>1,2</sup> to include repeated service loads. This article is an attempt to provide this extension by replacing the above plastic stress concentration factors with a new set of stress correction factors obtained from finite element analysis (FEA). These stress correction factors  $K$  are closely related to theoretical stress concentration factors (TSCFs), but as will be discussed later, they have the advantage of also accounting for the effect of the multiaxial state of stress at the failure location. The present results will provide design data of sufficient accuracy for preliminary sizing and circumvent the need to construct complex finite element models (FEMs) at an early design stage which, despite recent advances in computer hardware and software, can still be time-consuming and effort-intensive.

## Finite Element Model

A general-purpose finite element (FE) software COSMOS/M Ver 1.65A is used to generate the design data. Due to symmetry in loading and boundary conditions, a two-dimensional plane stress FEM comprising half the lug width  $W$  is used in the analyses. The loading and boundary conditions are shown in Fig. 2. Eight-noded isoparametric quadrilateral (quad) elements are used to model the lug.

Gap elements (also referred to as interface elements) are used to represent the contact interface between the lug and the pin that protrudes through the hole. The pin is not explicitly included in the FEM and its effect on lug deformations and stresses is simulated by the response of gap elements. Each of these elements is connected by two nodes and extends radially from the center to the boundary of the lug hole. Together they define the direction of the compressive force at the lug/pin interface. Should the lug deform in a way such that separation occurs between the pin and the lug, the FE solution automatically neglects the interface elements at the location where the separation occurs. The effect on lug stresses resulting from changes in the coefficient of friction  $\mu$  at the lug/pin interface is the subject of a separate investigation and

Received May 9, 1993; revision received May 30, 1993; accepted for publication Sept. 1, 1994. Copyright © 1994 by the American Institute of Aeronautics and Astronautics, Inc. All rights reserved.

\*Senior Stress Engineer, 1700 Business Center Drive; currently Member of Technical Staff, Jet Propulsion Laboratory, California Institute of Technology, 4800 Oak Grove Drive, Pasadena, CA 91109-8099. Senior Member AIAA.

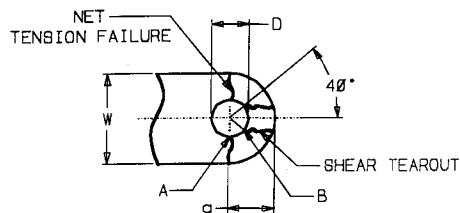


Fig. 1 Possible failure modes.

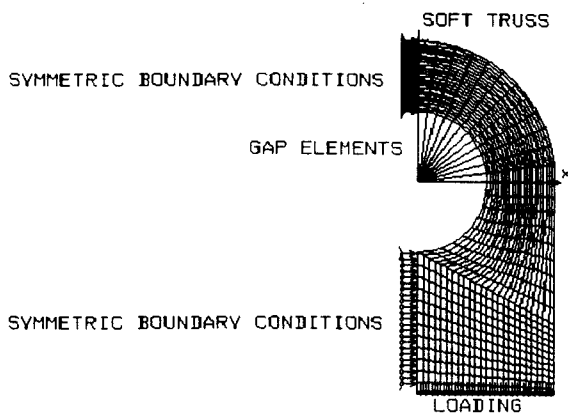


Fig. 2 Details of finite element model.

will be discussed later. In all analyses, a zero clearance condition is assumed at the lug/pin interface.

The gap elements are assumed rigid, which together with the constraint imposed by the present two-dimensional plane stress model, result in a uniform load and stress distribution through the lug thickness. In reality this may not necessarily occur, since possible bending of the interfacing pin may disrupt the even load distribution through the thickness. Since it is quite impossible to examine the entire range of lug/pin geometries, material combinations, and support configurations that occur in practice, it is necessary to assign a rigid interface to the FEM and account for the effect of pin flexibility by a separate analysis.

In addition to quad and gap elements, the FEM also includes a soft spring element (not shown in Fig. 2) to prevent numerical instability resulting from rigid body motion prior to the closure of gap elements.

Loading on all analyses is 1000 N and is distributed uniformly in the form of a pressure loading as shown in Fig. 2. A total of 17 different geometries with  $D/W$  ratios ranging from 0.1 to 0.9 in increments of 0.05 is analyzed. Values of "a" are kept constant at  $W/2$  (see Fig. 1). For all analyses,  $W$  is held constant at 25 mm, and the lug thickness  $t$  at 10 mm.

Material constants used in the FE analyses are based on steel with a value of 207 kN/mm<sup>2</sup> for  $E$  and 0.3 for  $\nu$ . The effect of material nonlinearity is not included. The reason for this omission will be discussed later. Stresses obtained from the present FE solutions are insensitive to changes in  $E$ , but do vary slightly with changes to  $\nu$ . However, for most aerospace alloys, including those of aluminum and titanium,  $\nu$  is relatively constant and does not deviate significantly from 0.3.

Failure is based on the distortion strain energy theory (also referred to as octahedral shear stress theory), which is generally accepted to be the most accurate fatigue failure criterion for most aerospace alloys.<sup>3</sup> This theory predicts failure to occur whenever the Von Mises stress  $f_v$  exceeds the fatigue strength of the material where  $f_v$  for a general stress state is given by:

$$f_v = \{0.5[(f_1 - f_2) + (f_2 - f_3) + (f_3 - f_1)]\}^{0.5} \quad (1)$$

where  $f_1$ ,  $f_2$ , and  $f_3$  are the principal stresses. For each geometry analyzed, values for  $f_v$  are recorded at initiation lo-

cations corresponding to the two different modes of failure (points A and B of Fig. 1).

### Convergence Study

Prior to the generation of design data, a convergence study is first performed to ensure that the mesh chosen for the analyses will achieve acceptable accuracies in reasonable computation times. The study is based on a  $D/W$  ratio of 0.1, which is a geometry that is expected to produce the highest stress gradient in the vicinity of the hole. A  $\mu$  of 0 is used in the present study.

Four different meshes ranging from 204 to 1408 quad elements (see Fig. 3) are used to calculate the stresses at locations A and B of Fig. 1. Results from these meshes are summarized in Fig. 4 where the percentage errors calculated by assuming the results from the finest mesh (mesh M4) to be the converged solution are plotted on the ordinate. Mesh M3 appears to offer the most logical compromise between accuracy and computation effort and is selected for all subsequent analyses with  $D/W$  ratio up to 0.6. For higher  $D/W$  ratios, the number of elements in the radial direction is progressively reduced and constantly monitored to ensure that the element aspect ratios in the vicinity of the hole are as near unity as possible.

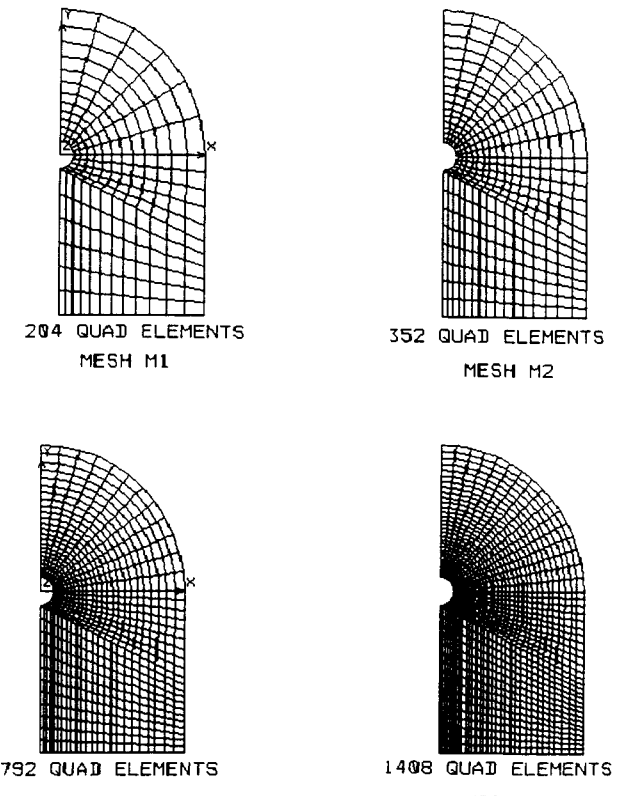
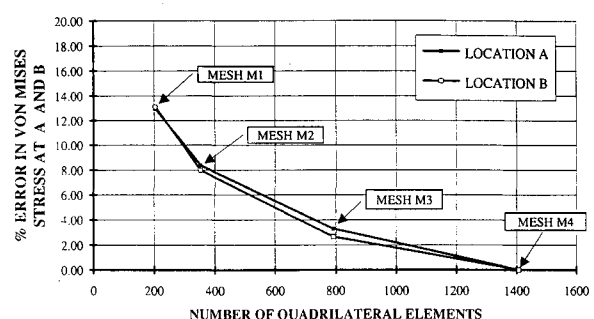


Fig. 3 Meshes used in convergence study.

Fig. 4 Results of convergence study ( $D/W = 0.1$ ).

## Discussion

From the FE results for  $D/W$  ratios of 0.1–0.9, stress correction factors  $K_{tn}$  and  $K_{br}$  corresponding to the tensile and shear-bearing modes of failure are derived. These factors are defined as

$$K_{tn} = f_{vA} A_{tn} / F \quad (2)$$

$$K_{br} = f_{vB} A_{br} / F \quad (3)$$

where  $f_{vA}$  and  $f_{vB}$  are the FE Von Mises stresses at points  $A$  and  $B$ , respectively (see Fig. 1),  $F$  is the axial load,  $A_{tn}$  and  $A_{br}$  are nominal tensile and shear-bearing areas given by

$$A_{tn} = (W - D)t \quad (4)$$

$$A_{br} = Dt \quad (5)$$

Variations of  $K_{tn}$  and  $K_{br}$  with changes in  $D/W$  ratios are shown in Fig. 5 for the case of  $\mu = 0$ . Other values of  $\mu$  are investigated later. The smoothness of these curves is a confirmation that all meshes used to produce the current results have achieved convergence. A design procedure and a worked example using these factors are described later. The stress correction factors are closely related to TSCFs since they also measure local stress increases due to geometry changes, but are more useful as failure indicators because they include the effect of combined stresses. It is important to note that values for  $K_{tn}$  can be substantially higher than 3, which despite only being applicable for the case of a hole in an axially loaded infinite plate, is unfortunately sometimes also assumed for the analysis of lugs. It is clear that the error introduced by such an assumption can be substantial. The reason for the stress concentration exhibiting such a large disagreement between the case of a lug and that of a perforated plate of infinite width is attributed to the difference in boundary conditions. For the lug, the restraint provided by the connecting pin causes all loads to flow very near the hole. This results in a much higher concentration of stress compared to the case of the infinite plate that has a more uniform load distribution, and only a relatively small portion of the total load is disrupted by the presence of the hole.

Apart from the inevitable numerical inaccuracies involved in the solution process, there are also other limitations associated with the FE solution, particularly the inability of the FE formulation to simulate the real material response under cyclical loading.<sup>4</sup> Most aerospace alloys are relatively ductile and depending on the stress level and number of load cycles, the full notch-sensitivity predicted by the present materially linear FE solutions may not occur, and the FE results may overpredict actual stresses. However, in practice, the surface surrounding the lug hole is sometimes treated by a case hardening process such as nitriding for wear protection, and the resultant brittle surface layer may indeed exhibit full notch sensitivity that would make the present FE stresses very realistic. Also, for high-cycle fatigue situations, stress levels are generally lower and local yielding (which is the primary reason

for reducing notch sensitivity), may not develop, and the FE stresses may again become very realistic.

The simulation of the notch-sensitivity effect by FEA is not attempted in practice, since apart from inputting the entire stress-strain curve for the material, the model must contain extremely high resolution. The resultant number of elements may be so large that the computation time involved for a nonlinear solution may become impractical. Since the intent of the present study is to provide design data for initial sizing, it is advantageous to omit the effect of plasticity so that the data may be applied to all Hookean materials. The effect of omitting plasticity will produce stress results that will err on the conservative side.

Other factors omitted by the present analyses include the effect of manufacturing tolerances, misalignment, and load eccentricity. These and other unavoidable uncertainties that occur in practice may cause the actual load and stress distribution to deviate somewhat from the FE results. In particular, any clearance between the lug hole and the connecting pin can further complicate the distribution of lug stresses. If the clearance is large enough, the two sides of the lug may deflect inward since no restraint is offered by the pin and may result in an additional increase in stress concentration. A common method of addressing all these uncertainties is to multiply the design load by a fitting factor  $C_f$ . A value of 1.15 for  $C_f$  has been suggested.<sup>1,2</sup>

A further limitation of the present FE approach lies in its inability to account for the effect of pin bending. The subject of pin failure is not addressed in this article, but for joints with relatively small pins or thick lugs, pin bending can cause an uneven load distribution through the thickness and result in higher stresses at the lug faces compared to the midlayer. A traditional approach of addressing this uneven stress distribution involves replacing the actual lug thickness with an active thickness.<sup>1,2</sup> A design procedure incorporating this approach will be described later.

The discussions above have focused on inaccuracies or limitations associated with the determination of lug stresses. A rational design must also account for the uncertainties related to material strength. The statistical variation of fatigue strength for many engineering alloys can be substantial and adequate life scatter factors should be applied to ensure the design meets the required level of structural reliability.<sup>4</sup> It is important to remember that fatigue data obtained from practical sources<sup>6,7</sup> are not generally corrected for scatter. In addition to statistical scatter, fatigue strengths may also need to be corrected for temperature, loading type, specimen size, surface finish, or other effects.

There are numerous factors that affect fatigue strength in general and their investigation is beyond the scope of this article. One factor that warrants special attention in the fatigue design of lugs is fretting which is a surface disturbance caused by small amplitude cyclic motion. In aircraft applications, fretting fatigue is particularly important as a failure mode because lugs are often subjected to tens of millions of small amplitude cycles. It is not yet possible to quantify the fatigue strength reduction due to fretting, since apart from lug stress level, many other factors are involved. The design consideration of fretting is further complicated by the fact that the extent of fatigue strength reduction often exhibits considerable scatter. The most effective strategy is to take precautions to reduce its likelihood of occurrence. Some of the more common measures that can be taken include careful material selection, provide surface treatment or coatings as lubricants, and the induction of compressive residual stresses at the contact interface by using interference fits.

The use of interference-fit bushings is a particularly effective design measure, since apart from inducing radial pressure to eliminate relative joint movement and, hence, fretting, residual tensile stresses induced in the lug itself result in a higher stress ratio  $R$  (ratio of minimum stress to maximum

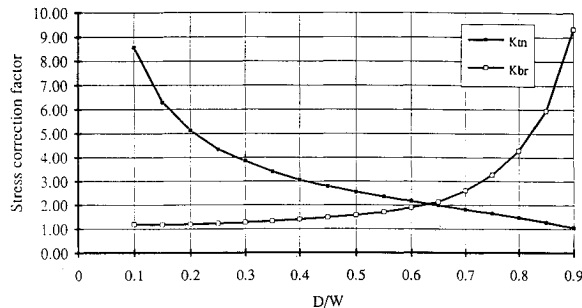


Fig. 5 Relationship between stress correction factors and  $D/W$ .

stress), which translates into longer service lives. However, the exact magnitude of the residual stresses is difficult to control and it is safe to use a stress ratio of zero in design.

Fatigue allowables are often presented in the form of *S-N* curves for a range of  $K$ , values. If the lug contains a smooth circular hole, a  $K$ , of 1 may be used since the stress concentration caused by the hole is already reflected by the curves in Fig. 5. However, if the lug contains additional geometric discontinuities such as a lubrication passage or slots for bearing installation, separate analyses should be conducted to evaluate the resultant stress concentration so that an appropriate value for  $K$ , may be selected for the calculation of margin of safety (MS).

In view of the large number of uncertainties and approximations related to the calculation of both stress and strength, the selection of a rational value for the MS is a particularly complex and difficult issue. MS is sensitive to analytical assumptions<sup>5</sup> and it is not possible to specify a value that is ideal for all situations. In aircraft application, weight is generally critical, and in view of the fact that lugs usually do not weigh much compared to the importance of their contribution to the overall structural integrity, a value of 0.2 has been suggested.<sup>1,2</sup>

### Effect of Friction

Up to this point, all analyses performed are based on a frictionless lug/pin interface ( $\mu = 0$ ). In this section, the effect of a varying  $\mu$  on lug stresses is investigated. A *D/W* lug geometry of 0.5 and a  $\mu$  range of 0–0.2 is chosen for the investigation. The determination of  $\mu$  for any design situation is an extremely complex exercise since friction is affected by many factors and is generally also a function of time. In practice, a bearing is often provided to reduce friction at the lug/pin interface. It is reasonable to expect that a properly designed and well-lubricated bearing under normal operating conditions will result in a  $\mu$  of less than 0.2.

The results are plotted in Fig. 6, where it may be seen that the variation of  $\mu$  within the present range does not have significant effects on the resultant stress correction factors. As  $\mu$  is increased,  $K_{br}$  exhibits a moderate decrease while  $K_{tn}$  increases very slightly. Based on these observations, the use of  $\mu = 0$  will produce the most balanced design and its selection for the generation of design data shown in Fig. 5 is justified.

It should be pointed out that the preceding conclusion regarding the effect of friction is applicable only to the present case of pure axial loading. For other load cases such as bending or transverse loads, there may be a tendency for lug rotation to occur and considerable bending forces may be generated by friction forces.

### Design Procedure

Based on the above discussions, the following design procedure is proposed. It should be noted that values for  $C_f$  and MS are not firm design limits. Other values should be used if they are supported by analytical or experimental justifica-

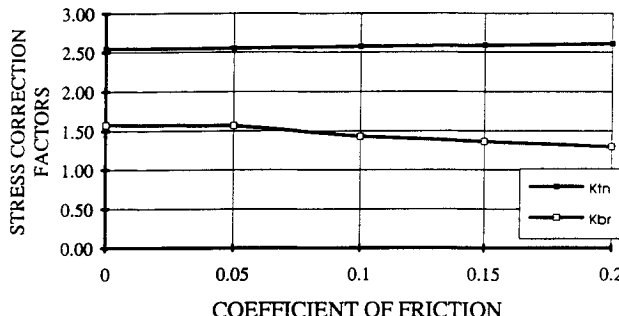


Fig. 6 Effect of friction on stress correction factors for *D/W* of 0.5.

tion or if they are superseded by design specification requirements:

- 1) Assume active lug thickness  $t_a$  to be equal to actual lug thickness  $t$ .
- 2) Calculate nominal tensile area  $A_{tn}$  and bearing area  $A_{br}$  as follows:

$$A_{tn} = (W - D)t_a$$

$$A_{br} = Dt_a$$

- 3) Calculate nominal tensile stress  $f_{tn}$  and nominal bearing stress  $f_{br}$ .  $C_f$  is a fitting factor normally assumed to be 1.15:

$$f_{tn} = C_f F/A_{tn}$$

$$f_{br} = C_f F/A_{br}$$

- 4) For the present *D/W* ratio, obtain stress correction factors  $K_{tn}$  and  $K_{br}$  from Fig. 5.

- 5) Calculate maximum tensile stress  $f_{tnmx}$  and maximum bearing stress  $f_{brmx}$ :

$$f_{tnmx} = K_{tn} f_{tn}$$

$$f_{brmx} = K_{br} f_{br}$$

- 6) Use larger value of  $f_{tnmx}$  and  $f_{brmx}$  to calculate MS. If MS < 0.2, the lug needs to be resized. Otherwise go to the next step.

- 7) Calculate margin of safety for pin bending based on a lug thickness of  $t_a$ . A method is proposed in Ref. 1.

- 8) If MS from step 7 is significantly larger than MS from step 6, lug sizing is satisfactory. Otherwise go to step 9.

- 9) Recalculate  $t_a$  using the method given in Ref. 1. Repeat steps 2–8. If step 8 cannot be satisfied, redesign with a larger pin.

### Example

A design example is presented to illustrate the application of the preceding procedure. In the lug joint depicted in Fig. 7 it is necessary to verify whether an inner lug thickness of 38 mm is capable of withstanding an axial load,  $F$  of 150,000 N for 10<sup>6</sup> cycles given that

Outer lug thickness  $t_1 = 20$  mm

Pin diameter  $D = 40$  mm

Inner lug width  $W = 50$  mm

Fatigue strength  $S$  of pin and inner lug = 800 N/mm<sup>2</sup>

Fitting factor  $C_f = 1.15$

Gap between inner and outer lugs  $g = 1$  mm

The design steps are as follows:

- 1) Assume  $t_a = 38$  mm
- 2)

$$A_{tn} = (50 - 40) \times 38$$

$$= 380 \text{ mm}^2$$

$$A_{br} = 40 \times 38$$

$$= 1520 \text{ mm}^2$$

3)

$$f_{tn} = 1.15 \times 150,000/380$$

$$= 453.95 \text{ N/mm}^2$$

$$f_{br} = 1.15 \times 150,000/1520$$

$$= 113.49 \text{ N/mm}^2$$

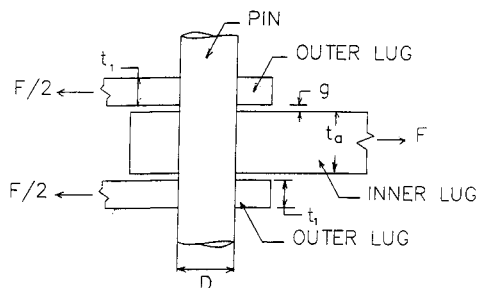


Fig. 7 Design example.

4) For a  $D/W$  ratio of 0.8,  $K_{tm} = 1.46$  and  $K_{br} = 4.28$  (see Fig. 5).

5)

$$f_{tmx} = 1.46 \times 453.95 \\ = 662.76 \text{ N/mm}^2$$

$$f_{brmx} = 4.28 \times 113.49 \\ = 485.74 \text{ N/mm}^2$$

6)

$$MS = (S/f_{tmx}) - 1 \\ = (800/662.76) - 1 \\ = 0.207$$

Since  $MS > 0.2$ , go to next step.

7) Pin bending lever arm

$$b = (t_1/2) + (t/4) + g \\ = (20/2) + (38/4) + 1 \\ = 20.5 \text{ mm}$$

Pin bending moment

$$M = Fb/2 \\ = 150,000 \times 20.5/2 \\ = 1,537,500 \text{ N/mm}$$

Second moment of area of pin

$$I = \pi D^3/64 \\ = 3.14159 \times 40^4/64 \\ = 125,663.6 \text{ mm}^4$$

Pin bending stress

$$f_p = \frac{MD}{2I} \\ = \frac{1,537,500 \times 40}{2 \times 125,663.6} \\ = 244.7 \text{ N/mm}^2$$

$$MS (\text{pin bending}) = (S/f_p) - 1 \\ = (800/244.7) - 1 \\ = 2.26$$

8) Since  $MS$  from step 7 is significantly larger than  $MS$  from step 6, the inner lug thickness of 38 mm is satisfactory.

### Conclusions

Based on analytical curves generated by two-dimensional plane stress FEA, a procedure for designing semicircular lugs under repeated axial loading is proposed. The curves relate stress correction factors from different failure modes to lug geometries and represent a simple and convenient alternative to constructing complex FEMs in the preliminary estimate of lug stresses. For the present axial loading, the effect of varying the coefficient of friction within the range of 0–0.2 at the lug/pin interface is found to have only minor influence on the stress correction factors. Pin bending and other practical limitations on the results are discussed. Difficulties associated with the accurate evaluation of lug strengths are also highlighted. Future investigation will include an extension of the present approach to the design of lugs of other shapes under axial and other loading conditions.

### References

- Melcon, M. A., and Hoblit, F. M., "Developments in the Analysis of Lugs and Shear Pins," *Product Engineering*, June 1953, pp. 161–170.
- Cozzone, F. P., Melcon, M. A., and Hoblit, F. M., "Analysis of Lugs and Shear Pins Made of Aluminum or Steel Alloys," *Product Engineering*, May 1950, pp. 113–117.
- Collins, J. A., *Failure of Materials in Mechanical Design*, Wiley, New York, 1981.
- Tsang, S. K., "Making Sense of FEA," *Machine Design*, March 26, 1993.
- Tsang, S. K., "A Statistical Procedure for Increasing Structural Efficiency," Society of Automotive Engineers TP 922037, 1992.
- Anon., "Metallic Material and Elements for Aerospace Vehicle Structures," Military Standardization Handbook, Dept. of Defense, June 1, 1987.
- Anon., "Aerospace Structural Metals Handbook," Metals and Ceramics Information Center, Batelle Columbus Lab.